Int. J. Sci. Res., Vol. 18 (2009), pp. 49-63

PALAEOSTRESS RECONSTRUCTIONS OF THE WADI HAM FAULT ZONE, NORTHERN OMAN MOUNTAINS, UNITED ARAB EMIRATES (UAE)

U. Zaineldeen[1,*] and A. Fowler[2]

[1,*]Department of Geology, Faculty of Science, Al Azhar University of Gaza,
P.O. Box 1277, Gaza, Palestine
(Corresponding Author: E-mail: u.zain@alazhar-gaza.edu)
[2]Geology Department, Faculty of Science, United Arab Emirates University,
P.O. Box 17551, Al-Ain, UAE
E-mail: afowler@uaeu.ac.ae

Keywords: Wadi Ham, Masafi, stress, tensor, strike-slip, compression.

ABSTRACT

This contribution is a detailed study of palaeostresses obtained by analysis of fault-slip data from the Wadi Ham Fault, between Masafi and Fujairah cities in the Northern Oman Mountains, United Arab Emirates (UAE). The study area forms the southwestern boundary of the Khor Fakkan massif – a block of mainly peridotitic and gabbroic rocks of the Semail Ophiolites, with in-faulted blocks of subophiolitic metamorphic sole. Palaeostress analysis confirms the subdivision of the tectonic evolution into four structural stages in terms of palaeostress regime. Stress inversion of fault-slip data was performed using an improved right-dieder method, followed by rotational optimization (TENSOR program). The results show that the area has been mainly controlled by strike-slip deformation. The fault-slip data yielded 15 distinct palaeostress tensors, distributed in different sites along the study area. Grouping of these tensors gives four structural stages. The first tensor (T1) stage is characterized by N-S to NNW-SSE S_{Hmax}. This stage produced NW-SE oriented dextral strike-slip faults, and NNE-SSW to NE-SW sinistral strike-slip faults. The >30 km long NW-SE trending dextral Wadi Ham Fault probably formed during this stage. The proposed age for T1 stage is late-obduction (Late Cretaceous). The next stage (T2) had S_{Hmax} trending NE-SW. At this stage the WNW-ESE to NW-SE sinistral strike-slip faults, NW-SE reverse faults and NE-SW normal faults were formed. The T2 tensor stage is also believed to be Late Cretaceous in age. The third stage (T3) had E-W S_{Hmax}. During this stage, NW-SE and NE-SW faults were reactivated as sinistral (or sinistral reverse oblique) and dextral strike-slip faults, respectively. The proposed age for T3 is Early Paleocene. The last tensor stage (T4) occurred in Paleocene to Early Eocene and was characterized by NW-SE S_{Hmax}. This stage created E-W reverse faults and NNW-SSE sinistral strike-slip faults, and reactivated NW-SE faults as normal faults.

INTRODUCTION

The Oman Mountains trend parallel to the Gulf of Oman in the southeastern part of the Arabian plate. These mountains formed in response to two main orogenic events in Late Cretaceous and mid-Tertiary. The first is represented by the Late Cretaceous (Coniacian to Maastrichtian) obduction of the Semail Ophiolite and associated sedimentary and volcanic rocks (Sumeini, Hawasina and Haybi groups) onto the eastern margin of the Arabian platform [1-10]. The second compressive event occurred in the Late Eocene to Miocene. It was responsible for the formation of foreland folds [11] and folding of Maastrichtian–Tertiary neoautochthonous units in the foredeep [7].

The study area is located in the northern part of the Oman Mountains, along Wadi Ham Fault, between Masafi and Fujairah cities, United Arab Emirates (Figure 1). Most of the study area is covered by Semail ophiolite and small areas of metamorphic sole rocks (Figure 1). The Semail Ophiolite of the Oman Mountains in eastern Arabia is the largest and best exposed thrust sheet of oceanic crust and upper mantle. It was emplaced onto the Arabian continental margin during Late Cretaceous time. The Semail Ophiolite has been studied by many authors, e.g. [1,2,3,5,8,9,10,12,13]. The Semail Ophiolite comprises strongly sheared and locally serpentinized peridotite. The peridotite has banded migmatites and gabbro intrusions. The base of the ophiolite is in contact with metamorphic sole amphibolites and greenschists along the Semail thrust. The contact between the peridotite and the metamorphic sole has been identified as a faulted contact. Many studies have been made on the structure and tectonics of the Northern Oman Mountains. The present study, however, focuses on the Wadi Ham Fault, for which no data on palaeostress evolution has previously been available. The tectonic structures of the study area have been described in details in Zaineldeen and Fowler (this volume). Our study investigates the palaeostress field in the Northern Oman Mountains in order to understand the tectonic history of the area. Therefore our results are the first to be reported for the Northern Oman Mountains, United Arab Emirates.

The study was carried out using satellite imagery, detailed studies of the structural features in the area and measurement of the structural elements to reconstruct the palaeostress tensors for the study area.

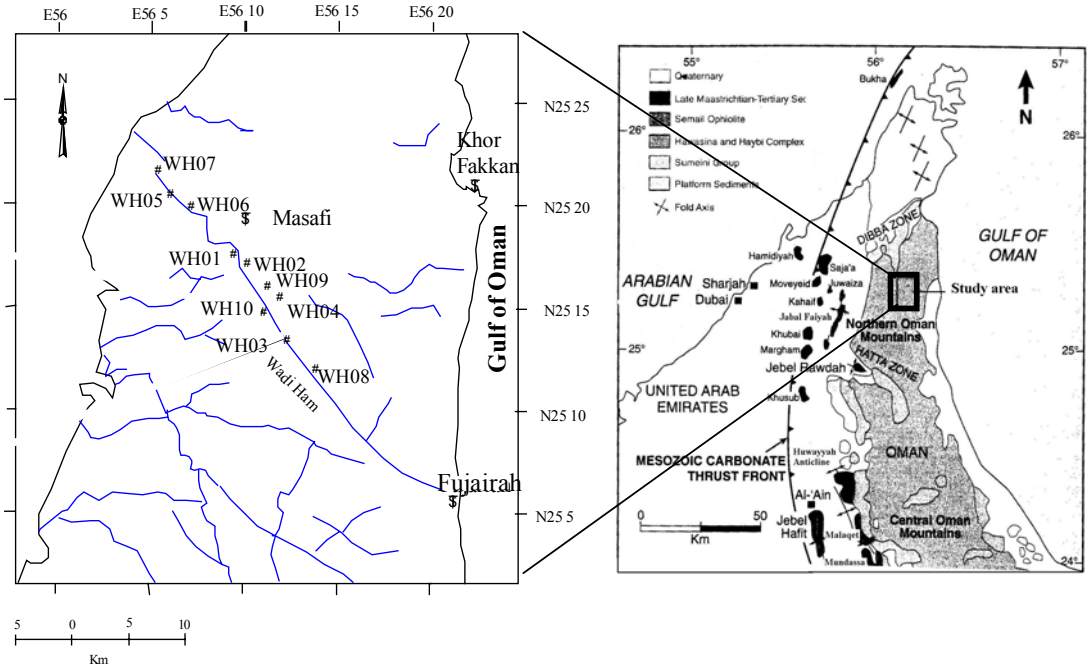

Fig. 1. Location of the established sites in the study area. See inset for location.

AIM OF THE STUDY

The study has been conducted along Wadi Ham Fault, Northern Oman Mountains, United Arab Emirates. The aims of the study are to:

1. measure and analyze the structural data from the field to obtain the palaeostress tensors;

2. reconstruct the kinematic and palaeostress evolution of the Northern Oman Mountains;

3. discuss the implications of our results for the origin of the Northern Oman Mountains.

STRUCTURAL ANALYSIS AND PALAEO-STRESS RECONSTRUCTION

Field investigation of fault kinematics was conducted along the Wadi Ham Fault. Palaeostress tensors were obtained by the application of a stress inversion technique on fault measurements. The results are presented and the relative chronology of the palaeostress stages is established when possible.

Fault plane, slip line orientation and sense of movement were used to compute the reduced stress tensors. The inversion is based on the assumption that the slip on a plane occurs in the direction of the maximum resolved shear stress [14], and that the apparent slip direction on the fault plane can be inferred from frictional grooves or slickensides. The fault-slip data were inverted to obtain the four parameters of the reduced stress tensor, as defined in [15]. These are the principal stress axes σ1 (maximum compression), σ2 (intermediate compression) and σ3 (minimum compression) and the ratio R of the principal stress differences: $R = (\sigma2- \sigma3)/(\sigma1- \sigma3)$. The two additional parameters of the full stress tensor are the ratio of extreme principal stress magnitudes (σ3/σ1) and the lithostatic load, but these cannot be determined from fault data alone. The first four parameters are determined successively using an improved version of the Right Dihedron method of [16] and a rotational optimization method, using the TENSOR program developed by [17,18].

During the rotational optimization, different functions can be optimized according to the nature of the tectonic structure.

For faults, the angular deviation between observed slip lines and computed shears is minimized, together with the maximization of friction coefficients for each fault plane. Not only can fault planes with slip lines be used for the reconstruction of stress tensors, but also tension and compression fractures.

The TENSOR procedure optimizes the appropriate function by progressive rotation of the tested tensor around each of its axes, and by testing different values of R. The amplitude of rotational angles and values of R ratio tested are progressively reduced until the tensor is stabilized. Separation of fault populations resulting from successive tectonic regimes is based on interactive kinematic separation and progressive stress tensor optimization, to obtain homogeneous subsets, representing different stress regimes.

The TENSOR program has been performed in many regions, e.g. [17,19,20,21,22]. The stress regime is determined by the nature of the vertical stress axes: extensional ($\sigma2\ S_{Hmax}$) when σ1 is vertical; strike-slip ($\sigma1\ S_{Hmax}$) when σ2 is vertical; and compressional ($\sigma1\ S_{Hmax}$) when σ3 is vertical. The stress regime can be expressed numerically by the stress regime index R' defined by [18,21] ranging from 0 to 3 as follows: R' = R when σ1 is vertical (extensional stress regime), R' = 2 – R when σ2 is vertical (strike-slip stress regime) and R' = 2 + R when σ3 is vertical.

Quality ranking has been defined by [18,23] throw the following criteria: number of fault-slip data (n) used in the inversion, ratio of fault-slip data used relative to the total number measured (n/nt), deviation between observed and theoretical slip directions (α_w) and slip sense confidence level for individual faults (Cl_w). These criteria are defined by TENSOR program. The quality ranking (Table 1) ranges from A (best) to E (worst).

The relative age of a stress tensor is determined from crosscutting relationships of striations and fault planes (fault-slip data).

Table (1). Quality ranking criteria for Stress tensor determination. n = number of fault-slip data used in the inversion, n/nt = ratio of fault-slip data used relative to the total number measured, α_w = deviation between observed and theoretical slip directions, CL_w = slip sense confidence level for individual faults [18,23].

Quality	n	n/nt	α_w	CL_w
A	≥25	≥0.60	≤9	≥0.70
B	≥15	≥0.40	≤12	≥0.55
C	≥10	≥0.30	≤15	≥0.40
D	≥6	≥0.15	≤18	≥0.25
E	<6	<0.15	>18	<0.25

PALAEOSTRESS ANALYSIS RESULTS

Minor faults with slip lines were measured in 10 different sites distributed along the study area. They were inverted to determine the palaeostress tensors according to the method described above. Sites are located on exposures of Semail Ophiolite and metamorphic sole. The stress inversion results allow the definition of four major palaeostress stages (T1-T4). The tensors are grouped according to their similarities as a function of stress axes orientation (S_{Hmax}) and stress regime index (R') as preferred by [18]. All obtained stress tensors are listed in Table 2 and displayed on maps for each of the palaeostress stage. Some sites exhibit more than one tensor, indicating that more than one stage occurred.

The palaeostress directions are as follows:

- T1: N-S to NNW-SSE S_{Hmax} strike-slip stress regime;
- T2: NE-SW S_{Hmax} strike-slip stress regime;
- T3: E-W S_{Hmax} compressive strike-slip (transpressional) stress regime;
- T4: NW-SE S_{Hmax} strike-slip stress regime.

S_{Hmax} for each stage was determined according to the World Stress Map data base [24]. For each group, the mean orientation of the stress axes (σ1, σ2 and σ3), the mean stress ratio and the stress regime index are presented in Table 2. The mean orientations of the three principal stress axes for each group are shown in Figure 2.

T1: N-S to NNW-SSE S_{Hmax}

The oldest structures recorded in the study area point to N-S to NNW-SSE directed compression. The calculated results are listed in Table 2. Four tensors have been obtained for this stage. Figure 3 shows plots for these tensors and illustrates the subset of the data together with the orientation of the calculated principal stress axes. All the stress tensors have sub-vertical σ2-axes and sub-horizontal σ1- and σ3-axes. The mean orientations of the principal stress axes are σ1 at 10/171, σ2 at 73/045 and σ3 at 13/263. The stress regime index R' is 1.44 indicating a strike-slip stress regime.

The results indicate a clear strike-slip regime (σ2 is vertical and σ1 and σ3 are horizontal) with a N-S maximum principal stress axis S_{Hmax} (σ1) and an E-W minimum principal stress axis S_{hmin} (σ3). All tensors for this stage are plotted on a map as shown in Figure 4.

Table (2). Palaeostress tensors from fault-slip data. Lat. = Latitude; Long. = Longitude; n = number of fault data used for stress tensor determination; nt = total number of fault data measured, n/nt = ratio of fault-slip data used relative to the total number measured; σ1, σ2 and σ3 = plunge and azimuth of principal stress axes; R = stress ratio (σ2- σ3)/ (σ1- σ3); α = mean slip deviation; Q = quality ranking; R' = stress regime index.

Site	Lat.	Long.	n	nt	n/nt	σ1	σ 2	σ 3	R	α	Q	R'	Tensor
T1: N-S to NNW-SSE S_{Hmax} (Late Cretaceous)													
WH02	25 16.4	56 10.3	11	62	0.18	33/152	56/348	08/247	0.56	11.49	C	1.44	Pure strike-slip
WH06	25 19.7	56 07.0	10	74	0.14	05/355	83/134	05/264	0.48	07.93	C	1.52	Pure strike-slip
WH07	25 21.1	56 05.2	13	51	0.25	15/158	52/048	34/259	0.67	11.67	D	1.33	Pure strike-slip
WH09	25 14.9	56 11.0	11	32	0.34	06/016	82/155	05/285	0.54	10.98	C	1.46	Pure strike-slip
Weighed mean			**45**	**219**		**10/171**	**73/045**	**13/263**	**0.56**			**1.44**	**Pure strike-slip**
T2: NE-SW S_{Hmax} (Late Cretaceous)													
WH02	25 16.4	56 10.3	17	62	0.28	09/235	71/351	16/142	0.57	07.49	B	1.43	Pure strike-slip
WH04	25 14.9	56 11.8	18	20	0.90	51/340	14/233	36/132	0.44	06.65	C	0.44	Pure extensive
WH06	25 19.7	56 07.0	07	74	0.10	06/053	79/291	09/144	0.61	11.55	D	1.39	Pure strike-slip
WH07	25 21.1	56 05.2	18	51	0.35	14/215	71/354	12/123	0.07	07.11	C	1.93	Comp. strike-slip
WH08	25 11.8	56 13.6	13	42	0.31	18/225	45/334	39/120	0.52	07.97	C	2.52	Oblique comp.
Weighed mean			**73**	**249**		**10/228**	**78/013**	**07/137**	**0.46**			**1.54**	**Pure strike-slip**
T3: E-W S_{Hmax} (Early Paleocene)													
WH01	25 16.5	56 9.3	18	49	0.37	21/264	69/073	03/172	0.55	06.83	B	1.45	Pure strike-slip
WH03	25 14.1	56 11.7	32	74	0.43	38/075	06/340	51/242	0.25	13.14	C	2.25	Pure compressive
WH09	25 14.9	56 11.0	12	32	0.37	26/113	55/338	22/215	0.41	07.58	C	1.59	Pure strike-slip
Weighed mean			**62**	**155**		**15/091**	**74/296**	**07/183**	**0.24**			**1.76**	**Comp. strike-slip**
T4: NW-SE S_{Hmax} (Paleocene to Early Eocene)													
WH03	25 14.1	56 11.7	26	74	0.35	32/131	17/031	53/276	0.60	10.20	B	2.60	Pure compressive
WH05	25 20.2	56 06.4	46	51	0.88	24/302	57/074	22/201	0.29	09.00	C	1.71	Comp. strike-slip
WH10	25 15.0	56 10.5	16	27	0.59	51/280	35/131	15/030	0.40	10.03	B	0.40	Pure extensive
Weighed mean			**88**	**152**		**15/128**	**74/283**	**07/036**	**0.43**			**1.57**	**Pure strike-slip**

T2: NE-SW S_{Hmax}

The second palaeostress stage represents five tensors. The results of these tensors are given in Table 2. The palaeostress tensors define a strike-slip regime with NE-SW σ1-orientation (S_{Hmax}). The mean orientations of the principal stress axes are σ1 at 10/228, σ2 at 78/013 and σ3 at 07/137. The results show that σ2 is vertical, σ1 and σ3 are horizontal and the stress regime index R' is 1.54, indicating strike-slip regime. The results are listed in Table 2 and Figure 5. All tensors for this stage are plotted on a structural map as shown in Figure 6.

T3: E-W S_{Hmax}

This stage represents three tensors obtained at three different sites distributed in the study area. These tensors are listed in Table 2 and shown in Figure 7. The calculated results show two tensors out of three are strike-slip regime and one is compressive stress regime. However the mean calculated tensor is compressive strike-slip (transpressional) stress regime with σ2 sub-vertical and σ1 and σ3 sub-horizontal. The mean orientations of the principal stress axes are σ1 at 15/091, σ2 at 74/296 and σ3 at 07/183. Figure 8 shows the projection of the three tensors at the three different locations in the study area.

T4: NW-SE S_{Hmax}

The last palaeostress stage affecting the study area has NW-SE S_{Hmax}. This stage is characterized by σ1 and σ3 being horizontal, σ2 vertical and a stress regime index R' of 1.57, indicating a typical strike-slip stress regime. Three tensors were obtained for this stage. The calculated results are listed in Table 2 and Figure 9. The mean orientations of the principal stress axes are σ1 at 15/128, σ2 at 74/283 and σ3 at 07/036. Figure 10 shows the projection of the two tensors for this stage.

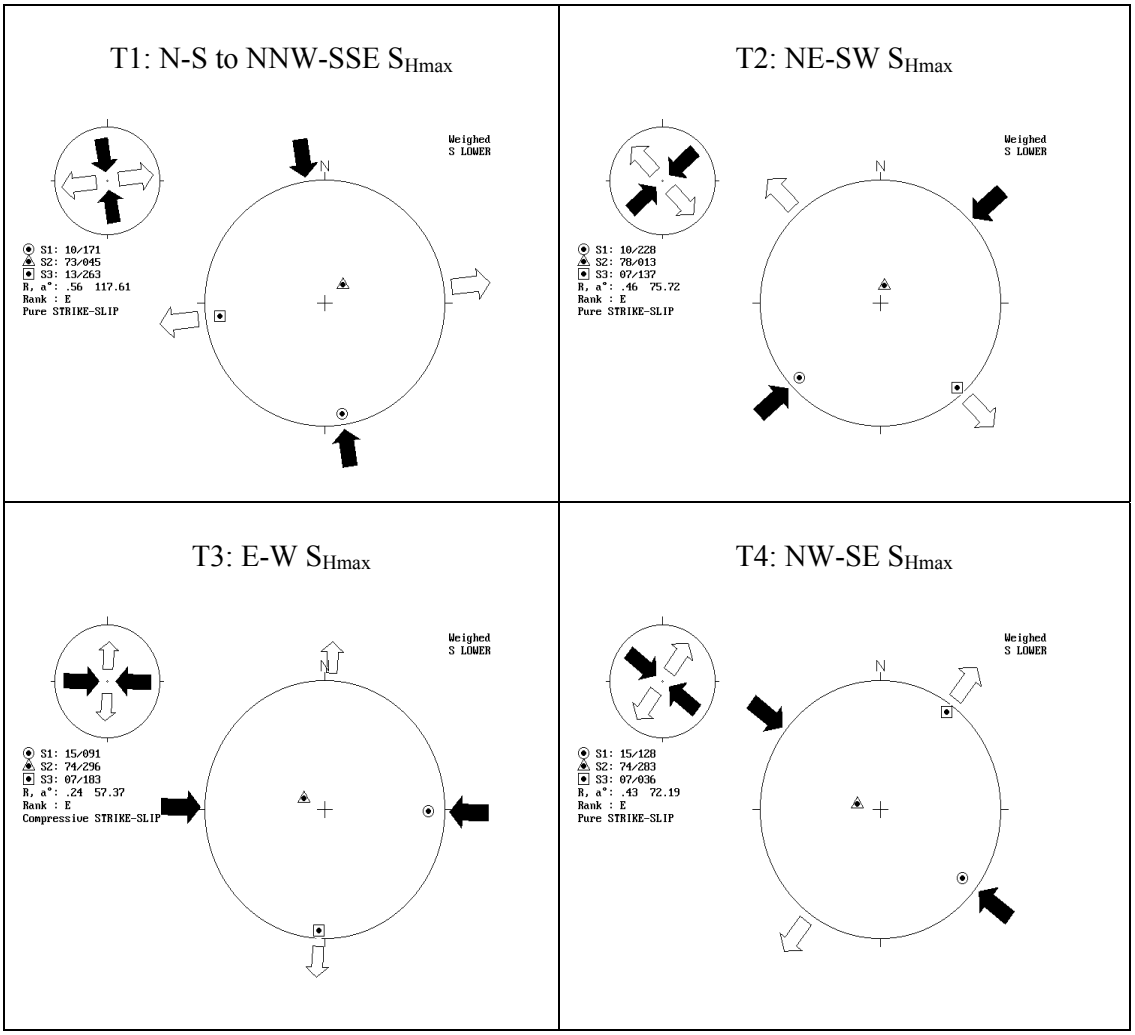

Fig. 2. Mean tensors for all tensor stages (T1-T4). Stereograms (Schmidt net, lower hemisphere) with trace of stress symbols (circles = σ1, triangles = σ2 and squares = σ3); S1, S2 and S3 = the three principal stress axes (σ1, σ2 and σ3 respectively); R = stress ratio.

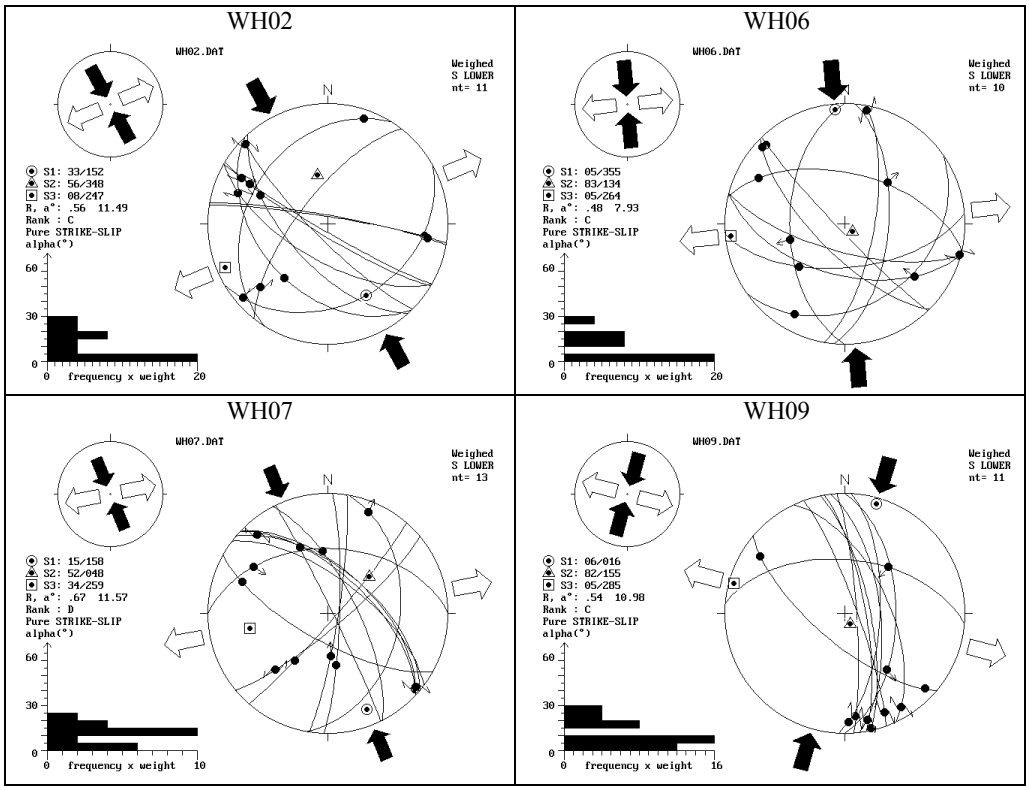

Fig. 3. Stress inversion results for T1 tensor stage (N-S to NNW-SSE S_{Hmax}). Stereograms (Schmidt net, lower hemisphere) with trace of fault planes, observed slip lines and slip sense; circles, triangles and squares = symbols of stress axes σ1, σ2 and σ3 respectively; S1, S2 and S3 = the three principal stress axes (σ1, σ2 and σ3 respectively); R = stress ratio; α = slip deviation; histogram of observed slip-theoretical shear deviation α for each fault plane.

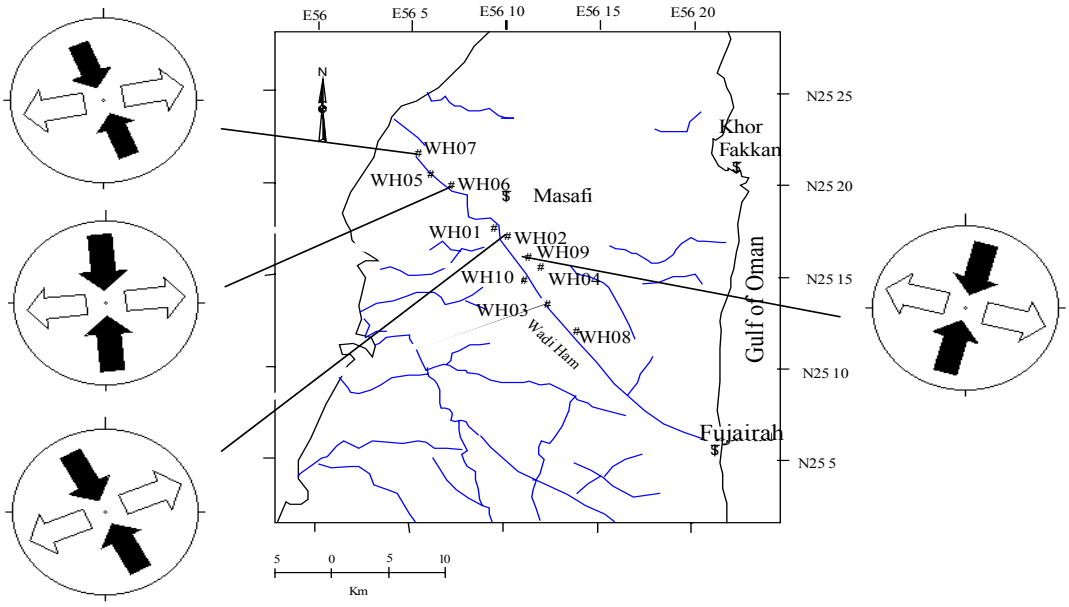

Fig. 4. Palaeostress tensors of the T1 stage (N-S to NNW-SSE S_{Hmax}) distributed at different sites along the study area.

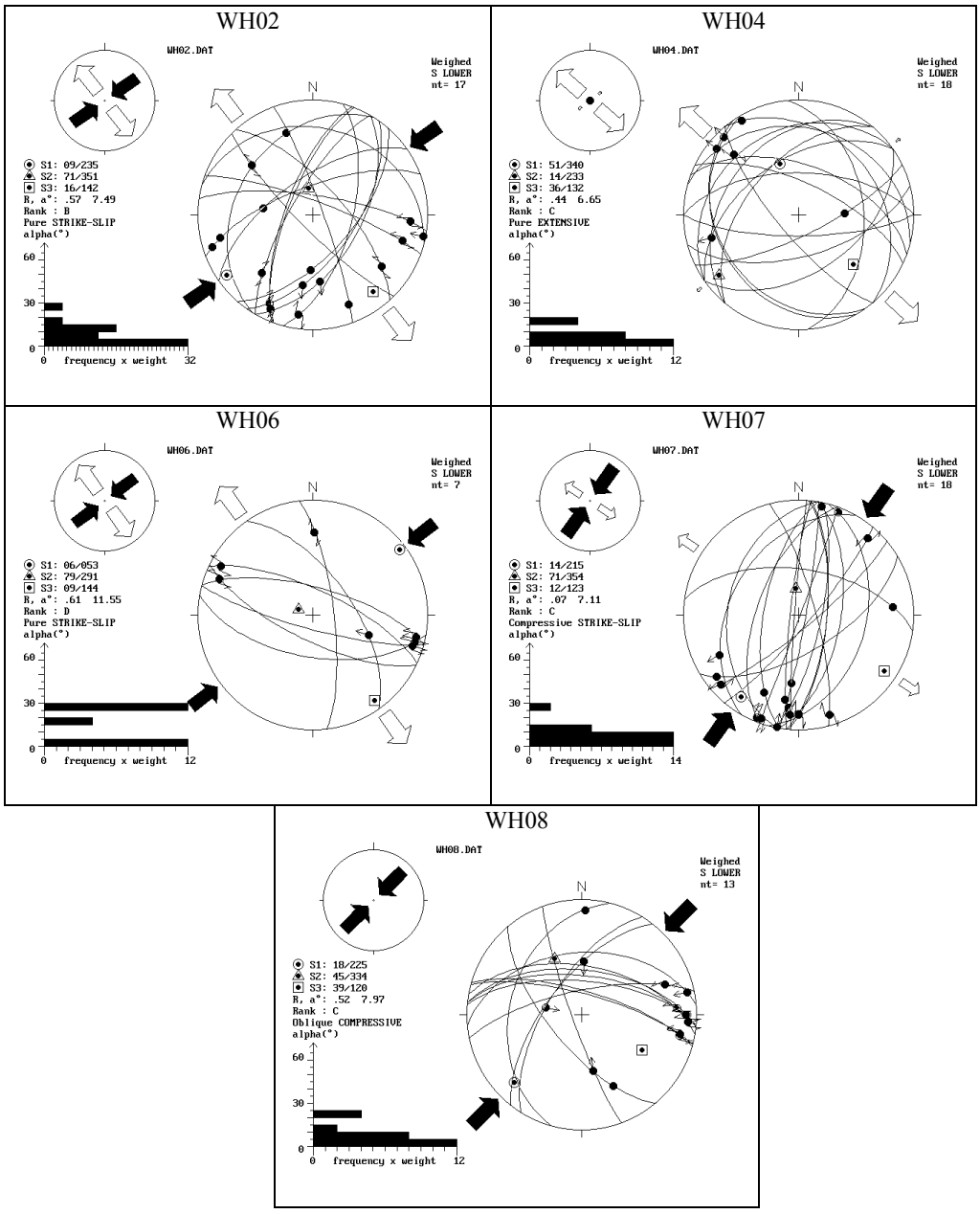

Fig. 5. Stress inversion results for T2 tensor stage (NE-SW S_{Hmax}). Stereograms as in Figure 3.

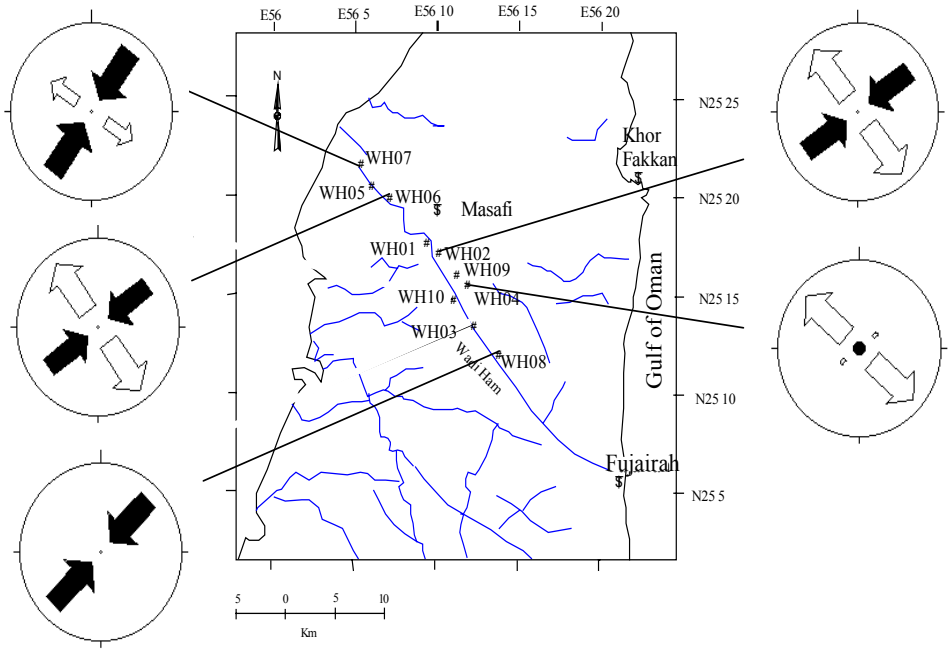

Fig. 6. Palaeostress tensors of the T2 stage (NE-SW S_{Hmax}) distributed at the sites along the area.

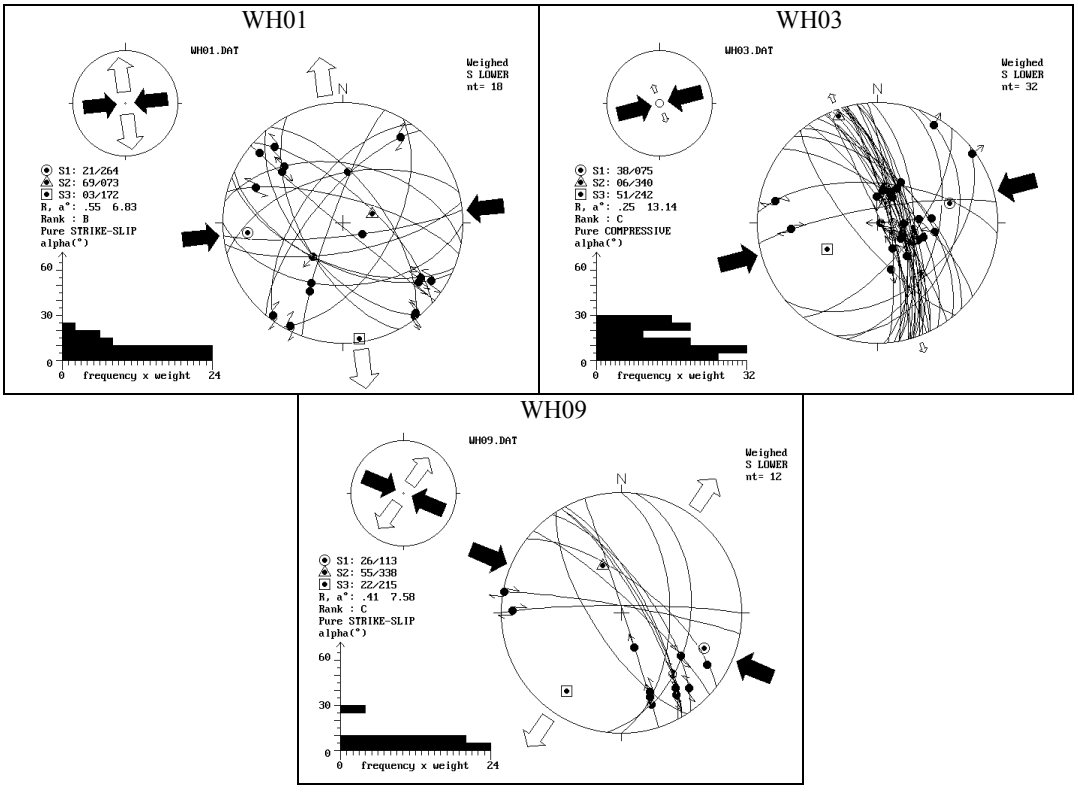

Fig. 7. Stress inversion results for T3 tensor stage (E-W S_{Hmax}). Stereograms as in Figure 3.

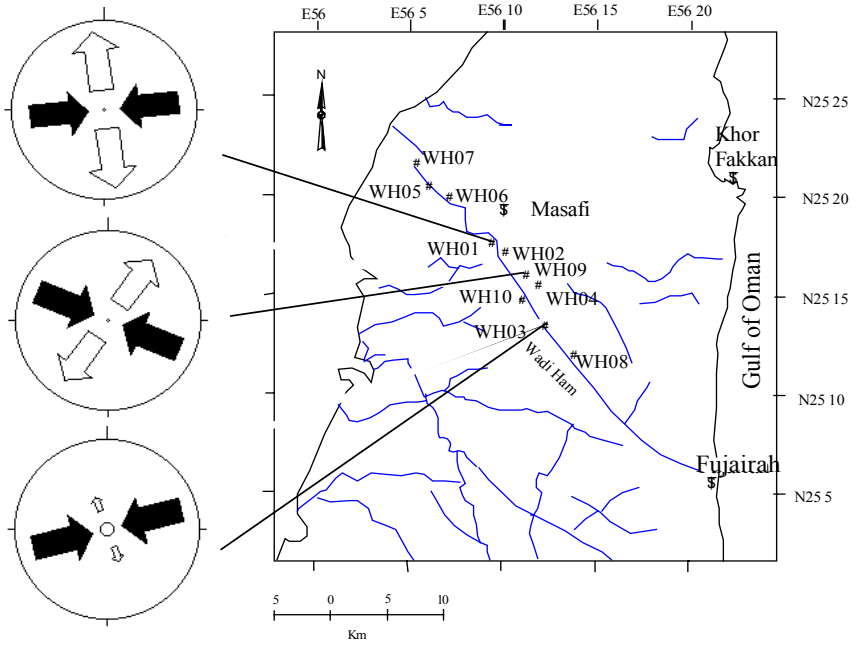

Fig. 8. Palaeostress tensors of the T3 stage (E-W S_{Hmax}) distributed at different sites along the area.

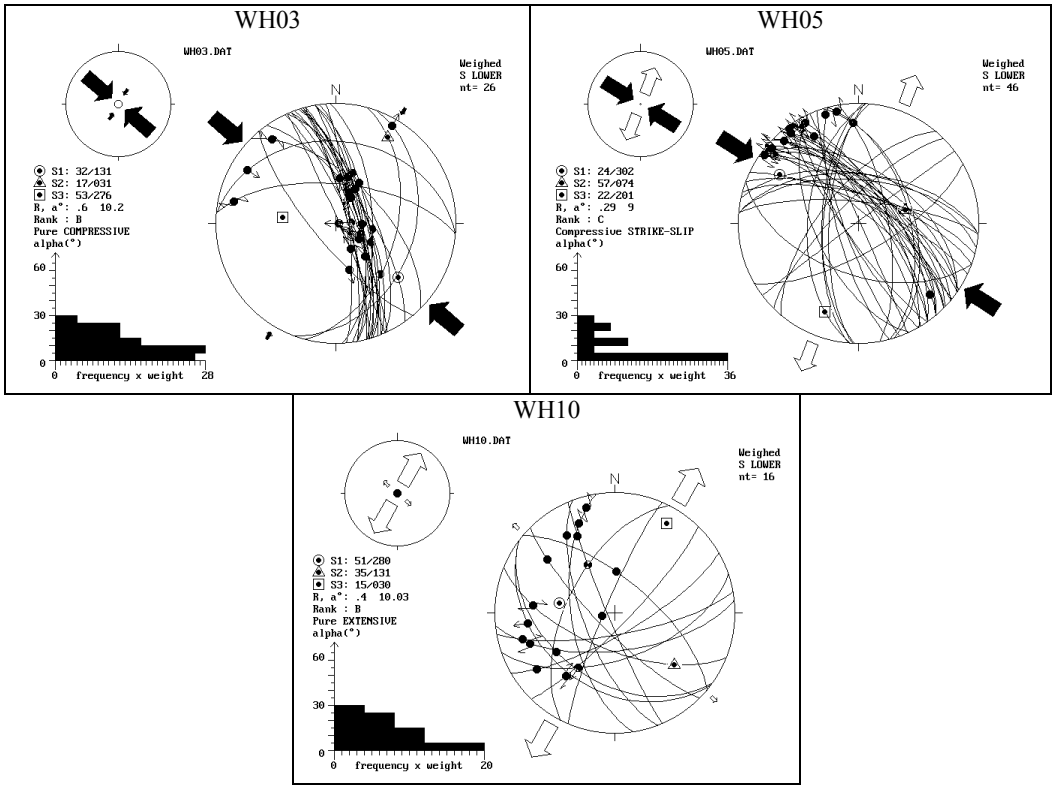

Fig. 9. Stress inversion results for T4 tensor stage (NW-SE S_{Hmax}). Stereograms as in Figure 3.

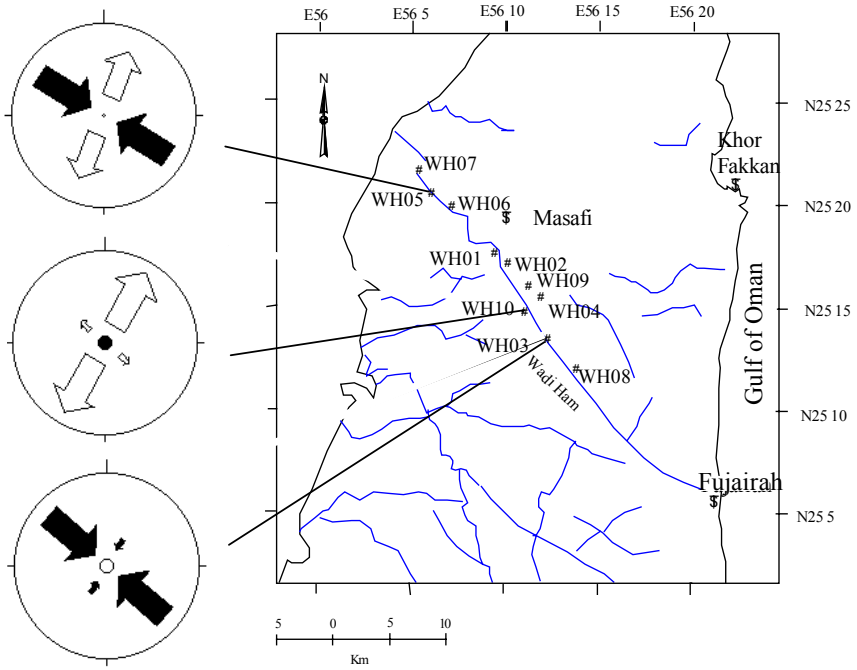

Fig. 10. Palaeostress tensors of the T4 stage (NW-SE S_{Hmax}) distributed at the sites along the area.

DISCUSSION

The present study presents the first palaeostress results obtained from kinematic slip data along Wadi Ham Fault, between Masafi and Fujairah cities in the Northern Oman Mountains, United Arab Emirates. The fault slip data used for reconstructing the stress field allows characterization of the palaeostress field. They also allow analysis of the kinematics of the movements along the faults at different geological stages. The main objectives of the study were (1) to construct the palaeostress tensors along the Wadi Ham Fault; (2) to provide a palaeostress analysis; (3) to better understand the evolution of the Northern Oman Mountains. The results of the stress inversion lead us to conclude that the study area was subjected to several different stress events since Late Cretaceous times.

Four major palaeostress regimes (T1-T4) have been recognized. They are of a strike-slip type, with horizontal principal compression. They differ mainly by the orientation of their principal axis of compression (σ1). According to crosscutting relationships of striations and fault planes (fault slip data), the palaeostress stages have been successively classified into: (T1) N-S to NNW-SSE S_{Hmax}; (T2) NE-SW S_{Hmax}; (T3) E-W S_{Hmax}; and (T4) NW-SE S_{Hmax}. The structural elements of these stages are compatible with those described in different areas elsewhere in Northern Oman Mountains [11,25,26]. Hence the age of our stages are as follows: T1 is Late Cretaceous in age, T2 is also Late Cretaceous in age but older than T1, T3 is Early Paleocene and T4 is Paleocene to Early Eocene in age. The sequence of stages and their age constraints are discussed below.

T1: N-S to NNW-SSE S_{Hmax}

The earliest tectonic stage affecting the study area is characterized by a strike-slip stress regime with a maximum horizontal principal stress axis (S_{Hmax}) oriented N-S. This stage produced NW-SE oriented dextral strike-slip faults and NNE-SSW to NE-SW sinistral

strike-slip fault. The >30 km long NW-SE trending dextral Wadi Ham Fault was formed during this stage.

The Oman Mountains are the product of two distinct orogenies. The first one occurred during Late Cretaceous (Senonian). The second orogeny, which began in the Miocene and continued to the present, was related to the Zagros collision [27,28]. The T1 tectonic stage is related to the first orogeny. Warrak [25] reported four phases of deformation that affected the southern part of the Northern Oman Mountains front during the Late Cretaceous. The first phase includes the emplacement of the allochthonous units (Hawasina, Haybi and Semail Ophiolites) in the form of thrust sheets. We believe that our T1 tectonic stage is related to the first stage proposed by [25] due to compatibility of the structures in both stages. Therefore, the T1 tectonic stage affected the study area during Late Cretaceous.

T2: NE-SW S_{Hmax}

This stage is also characterized by a strike-slip stress regime like T1 but with a different orientation of S_{Hmax}. The orientation of S_{Hmax} for this stage is NE-SW. This direction is well constrained from five stress sites. This stage caused sinistral strike-slip faults trending WNW-ESE to NW-SE, reverse faults trending NW-SE and normal faults trending NE-SW.

The maximum principal stress axis for this stage is compatible with SW-directed exhumation and NE-directed subduction during the ophiolite obduction. The obduction of the Semail Ophiolite took place during the Late Cretaceous [1,3,7]. The direction of compression of the T2 stage is parallel to the direction of the emplacement of Semail Ophiolite. The contact is a thrust that caused by NE-SW compression. So, we propose that the T2 tectonic stage is related to the obduction that formed during Late Cretaceous but younger than the T1 stage.

T3: E-W S_{Hmax}

The palaeostress analysis indicates that this stage is characterized by a compressive strike-slip (transpressional) stress regime (R' = 1.76) with a subhorizontal (15/091) orientation for the maximum principal stress axis (S_{Hmax}). During this stage, NW-SE and NE-SW faults were reactivated as sinistral (or sinistral reverse oblique) and dextral strike-slip faults, respectively.

Tertiary deformation caused major tectonism in the area, thus reactivating Late Cretaceous structures, mainly faults. In the Mid-Tertiary, the collision of the Arabian plate with Iran initiated a second phase of thrusting and folding of the Oman Mountains with the same age as the thrusting in the Zagros Mountains of Iran [11]. The direction of shortening was E-W due to this collision. Noweir and Eloutefi [29] believe that the NNW-SSE Malaqet – Mundassa fold southeast of Al-Ain (Figure 1) developed during the Late Cretaceous – Late Tertiary time. The direction of this fold is compatible to the direction of the maximum principal stress axis of the T3 stage (E-W S_{Hmax}). Noweir & Alsharhan [30] reported that the Huwayyah Anticline (Figure 1) that trends NNW-SSE northeast of Al-Ain formed in post-Middle Eocene time. The trend of this fold suggests E-W compression. This direction is compatible to our T3 stage (E-W S_{Hmax}). It is also compatible to the third deformational phase proposed by [25] that produced minor and major folds trending generally in NNW-SSE direction. This deformation developed during a long period of time, starting just before the Late Maastrichtian and lasting until after the Miocene. Abd-Allah [26] reported the third tectonic phase in Jabal Al Fayah area (southwest of Masafi, Figure 1) to be placed in Early Paleocene time. Therefore, an Early Paleocene age for the T3 tectonic stage is proposed.

T4: NW-SE S_{Hmax}

The palaeostress results show that this stage is characterized by a strike-slip stress regime. The maximum principal stress axis S_{Hmax} for this stage is oriented NW-SE. This stage is constrained by stress tensors from three separate location sites. This stage created E-W reverse faults and NNW-SSE sinistral strike-slip faults, and reactivated NW-SE faults as normal faults.

According to our results, T4 stage represents the last tectonic stage affecting the study area. Abd-Allah [26] reported a NW-SE compressional phase that caused the Al Fayah

Fold Belt (Figure 1). This compression took place at the Late Paleocene – Early Eocene boundary. This direction of compression is widespread along the western margin of the Oman Mountains [2,11,31,32]. So, the proposed age for our T4 tectonic stage is Paleocene to Early Eocene.

Due to the lack of differing lithologies in the study area and because the study area is restricted to the Semail Ophiolites, definite ages for the different tectonic stages are difficult to determine. So, we relate our stress stages to other tectonic stages, which have similar structures, elsewhere in the Northern Oman Mountains.

CONCLUSION

This study has detailed the tectonic evolution of the Wadi Ham area, Northern Oman Mountains, United Arab Emirates in terms of four deformation stages and related stress fields. This sequence of tectonic regimes has been established from microtectonic observations and structural studies on faults. They are characterized by the following succession of stress fields:

1. Late Cretaceous N-S to NNW-SSE S_{Hmax}, strike-slip stress regime;
2. Late Cretaceous NE-SW S_{Hmax}, strike-slip stress regime;
3. Early Paleocene E-W S_{Hmax}, compressive strike-slip (transpressional) stress regime;
4. Paleocene to Early Eocene NW-SE S_{Hmax}, strike-slip stress regime.

The first two stages (T1 and T2) reflect tectonic regimes of Late Cretaceous structures. T1 (N-S to NNW-SSE S_{Hmax}) has a strike-slip stress regime and corresponds to the major NW-SE trending faults, Wadi Ham Fault being one of them. T2 (NE-SW S_{Hmax}) has also a strike-slip stress regime but is younger than the T1 stage. T3 reflects the tectonic stress regime of Early Paleocene structures. T3 (E-W S_{Hmax}) has a compressive strike-slip (transpressional) stress regime and corresponds to the reactivation of Late Cretaceous structures and formation of folds elsewhere outside the study area within the Northern Oman Mountains.

T4 (NW-SE S_{Hmax}) has a strike-slip stress regime and corresponds to the formation of strike-slip and reverse faults and involved reactivation of the existing faults in the area. It also corresponds to the formation of folds in the region.

ACKNOWLEDGEMENT

The authors wish to thank the United Arab Emirates University for financial support given to Usama Zaineldeen for his stay in Al Ain while conducting field work, and for providing transportation to the field. They also thank Al Azhar University – Gaza, Gaza, Palestine, for providing financial support for transportation to the United Arab Emirates.

REFERENCES

1. K. W. Glennie, M. G. A. Boeuf, M. W. Hughes Clark, M. Moody-Stuart, W. F. H. Pilaar and B. M. Reinhardt, Late Cretaceous Nappes in Oman Mountains and their geologic evolution, *American Association of Petroleum Geologists Bulletin*, **57**, 5-27 (1973).
2. K. W. Glennie, M. G. A. Boeuf, M. W. Hughes Clark, M. Moody-Stuart, W. F. H. Pilaar and B. M. Reinhardt, Geology of the Oman Mountains, *Verhandelingen Koninklijk Nederlands Geologisch Mijnbouwkundig Genootschap*, **31**, 423 (1974).
3. R. G. Coleman, Tectonic setting for Ophiolite obduction in Oman, *Journal of Geophysical Research*, **86**, 2497-2508 (1981).
4. M. P. Searle, N. P. James, T. J. Calon and J. D. Smewing, Sedimontological and structural evolution of the Arabian Continental Margin in the Musandam Mountains and Dibba Zone, United Arab Emirates, *Geological Society of American Bulletin*, **94**, 1381-1400 (1983).
5. S. J. Lippard, A. W. Skelton and I. G. Gass, The Ophiolite of Northern Oman, *Geological Society of London Memoir*, **11**, 1-178 (1986).

6. S. C. Nolan, B. P. Clissold, J. D. Smewing and P. W. Skelton, Late Campanian to Tertiary Palaeogeography of the Central and Northern Oman Mountains. In Symposium on the Hydrocarbon Potential on Intense Thrust Zones. Ministry of Petroleum and Mineral Resources, *UAE and OPEC, Kuwait, Abu Dhabi*, 175-200 (1986).

7. D. R. D. Boote, D. Mou and R. I. Waite, Structural Evolution of the Suneinah Foreland, Central Oman Mountains. In Robertson A.H.F., Searle, M.P. & Ries, A.C. (Eds), The Geology and Tectonics of the Oman Region, *Geological Society of London*, Special Publication No. **49**, 397-418 (1990).

8. A. H. F. Robertson, A. E. S. Kemp, D. C. Rex and C. D. Blome, Sedimentary and Structural Evolution of Continental Margin Transform Lineaments: The Hatta Zone, Northern Oman Mountains. In Robertson A.H.F., Searle, M.P., Ries, A.C. (Eds), The Geology and Tectonics of the Oman Region, *Geological Society of London*, Special Publication No. **49**, 285-305 (1990).

9. M. P. Searle, R. R. Parrish, C. J. Warren and D. J. Waters, Structural evolution, metamorphism and restoration of the Arabian continental margin, Saih Hatat region, Oman Mountains, *Journal of Structural Geology*, **26**, 451-473 (2004).

10. C. J. Warren, R. R. Parrish, M. P. Searle and D. J. Waters, Dating the geologic history of Oman's Semail Ophiolite; insights from U/Pb geochronology, *Contributions to Mineralogy and Petrology*, **150**, 403-422 (2005).

11. M. Warrak, Origin of the Hafiat Structure: Implications for timing the Tertiary Deformation in the Northern Oman Mountains, *Journal of Structural Geology*, **18**, 803-818 (1996).

12. A. Nicolas, G. Ceuleneer, F. Boudier and M. Misseri, Structural mapping in the Oman ophiolites: Mantle diapirism along an oceanic ridge, *Tectonophysics*, **151**, 27-56 (1988).

13. M. P. Searle and J. S. Cox, Tectonic setting, origin and obduction of the Oman ophiolite, *Geological Society of American Bulletin*, **111**, 104-122 (1999).

14. M. H. P. Bott, The mechanism of oblique slip faulting, *Geological Magazine*, **96**, 109-117 (1959).

15. J. Angelier, From orientation to magnitudes in paleostress determinations using fault slip data, *Journal of Structural Geology*, **11**, 37-50 (1989).

16. J. Angelier and P. Mechler, Sur une méthode graphique de recherche des contraintes principales également utilisable en tectonique et en séismologie: 1a méthode des dièdres droits, *Bull. Soc. Géol. France*, **67(19)**: 1309-1318 (1977).

17. D. Delvaux, The TENSOR program for palaeostress reconstruction: examples from the East African and the Baikal rift zones, Terra Abstract, *Abstract Supplement,* No.**1**, to Terra Nova, **5**, 216 (1993).

18. D. Delvaux and B. Sperner, Stress tensor inversion from fault kinematic indicators and focal mechanism data: the TENSOR program. In: New Insights into Structural Interpretation and Modeling (D. Nieuwland Ed.), *Geological Society, London*, Special Publication, **212**, 75-100 (2003).

19. D. Delvaux, R. Moeys, G. Stapel, A. Melnikov and V. Ermikov, Paleostress reconstruction and geodynamics of the Baikal region, Central Asia. Part I:Paleozoic and Mesozoic pre-rift evolution, *Tectonophysics*, **252**, 61-101 (1995).

20. D. Delvaux, R. Kervyn, E. Vittori, R. S. A. Kajara and E. Kilembe, Late Quaternary tectonic activity and lake level fluctuation in the Rukwa rift basin, East Africa, *Journal of African Earth Sciences*, **26(3),** 397-421 (1997a).

21. D. Delvaux, R. Moeys and G. Stapel *et al*., Paleostress reconstruction and geodynamics of the Baikal region, Central Asia. Part II: Cenozoic tectonic stress and fault kinematics, *Tectonophysics*, **282(1-4)**, 1-38 (1997b).

22. U. Zaineldeen, D. Delvaux and P. Jacobs, Tectonic evolution in the Wadi Araba segment of the Dead Sea Rift, South-West Jordan, *European Geophysical Society*, Special Publication Series, **2**, 63-81 (2002).

23. B. Sperner, B. Muller, O. Heidbach, D. Delvaux, J. Reinecker and K. Fuchs, Tectonic Stress in the Earth's Crust: Advances in the World Stress Map Project. In: New Insights into Structural Interpretation and Modeling (D. Nieuwland Ed.)., *Geological Society, London*, Special Publication, **212**, 101-116 (2003).

24. B. Muller, B. Sperner, U. Theune and K. Fuchs, The World Stress Map Project (WSM), Heidelberg Academy of Science and Humanities, *Geophysical Institute, University of Karlsruhe, Germany* (1997).

25. M. Warrak, Structural evolution of the northern Oman Mountains front, Al Ain region, In Hydrocarbon potential of intense thrust zones *(Proceeding of Abu Dhabi Symposium) Kuwait*, **1**, 375-391 (1986).

26. A. M. A. Abd-Allah, Folding and faulting of neoautochthonous sequences in the Al Fayah Fold Belt: Northern Oman Mountains, United Arab Emirates, *Annals of the Geological Survey of Egypt*, **XXIV**, 413-433 (2001).

27. M. P. Searle, Sequence of thrusting and origin of culmination in the northern and central Oman Mountains, Journal *of Structural Geology*, **7**, 129-143 (1985).

28. M. P. Searle, Thrust tectonics of the Dibba zone and the structural evolution of the Arabian continental margin along the Musandam Mountains (Oman and United Arab Emirates), *Journal of the Geological Society, London*, **145**, 43-53 (1988).

29. A. M. Noweir and N. S. Eloutefi, The structural and stratigraphy of Jabal Malaqet – Jabal Mundassa area, Southeast Al-Ain, Northern Oman Mountains, United Arab Emirates, *Neues Jahrbuch fur Geologie und Paläontologie, Abhandlungen*, **204**, 263-284 (1997).

30. A. M. Noweir and S. Alsharhan, Structural Style and Stratigraphy of the Huwayyah Anticline: an Example of an Al-Ain Tertiary Fold, Northern Oman Mountains, *GeoArabia*, **5(3),** 387-402 (2000).

31. Hunting Geology and Geophysics Limited, Report on a Mineral Survey of the U.A.E., Al-Ain Area, *Ministry of Petroleum and Mineral Resourecs, Abu Dhabi*, **9**, 1-29 (1979).

32. O. H. Cherif and W. M. Z. El Deeb, The Middle Eocene-Oligocene of the northern Hafit area, south of Al Ain City (United Arab Emirates), *Geol. Medit*., **11**, 207-217 (1984).